Canadian Journal of
**Fisheries and
Aquatic Sciences**

Research Article

Darkening waters: climate-induced shifts in precipitation and DOM reduced phytoplankton but not zooplankton in dimictic boreal lakes

Scott N. Higgins[a], **Sonya M. Havens**[a], **Michael J. Paterson**[a], **M. Rennie**[a,b], **and P. Bulloch**[a]

[a]International Institute for Sustainable Development Experimental Lakes Area, Winnipeg, MB R3B 0T4, Canada; [b]Department of Biology, Lakehead University, Thunder Bay, ON P7B 5E1, Canada

Corresponding author: **Scott N. Higgins** (email: shiggins@iisd-ela.org)

Abstract

This study examines the extent to which temporal (1980–2019) increases in precipitation drove dissolved organic matter (DOM) loads and lake concentrations, and evaluates implications to physical, chemical, and biological variables within dimictic boreal lakes at the IISD Experimental Lakes Area, Canada. Long-term increases in precipitation (c. +27%) were associated with increased DOM loads and lake concentrations (c. +9%). Increased DOM within dimictic lakes over time was associated with shallower thermocline depths (c. −17%) and euphotic depths (c. −13%), reduced mean light intensity in the water column (c. −20%), reduced depth-integrated phytoplankton biomass (c. −32%) but increased epilimnetic chlorophyll *a* concentration (c. + 27%), and we detected no significant temporal declines in crustacean zooplankton. Our results confirm earlier observations that caution should be exercised when using epilimnetic chlorophyll *a* as an indicator of phytoplankton responses to DOM. However, once corrected for photoadaptation depth-integrated chlorophyll *a* was a useful indicator of depth-integrated biomass and its response to DOM.

Key words: climate change, dissolved organic carbon, light, phytoplankton, zooplankton, food web

Introduction

A central tenet of the nutrient colour paradigm is that, by itself, information on the trophic status of lakes is insufficient to characterize lake ecosystems and their response to a wide range of drivers including organic contaminants, UV radiation, recovery from acid rain, climate change, and many others. To more accurately characterize lake ecosystems and their responses to such drivers, information on dissolved organic matter (DOM) is also necessary (Williamson et al. 1999). Though not exclusively, an important reason for the inclusion of DOM is related to its effect on light availability and associated effects on whole lake primary production and the productivity of higher trophic levels. While not all DOM is highly chromophoric, humic and fulvic components of allochthonous DOM have strong light attenuating properties and in many regions, including the boreal ecozone, DOM has strong effects on water clarity (Weyhenmeyer et al. 2016). Spatially, DOM varies considerably among lakes, even those in close proximity. Lake surveys have reported a range in DOM concentrations from <1 to >40 mg dissolved organic carbon (DOC) L^{-1} (Williamson et al. 1999; Webster et al. 2008; Sherbo et al. 2023) and many studies have documented how these spatial gradients of DOM have large and ecologically significant effects on physical properties (e.g., light availability, thermocline depth), chemical properties (e.g., nutrient availability, CO_2 evasion), and lake food webs from microbes to fish (Solomon et al. 2015; Creed et al. 2018). In general, most space-for-time (i.e., among lake) studies demonstrate that increases in DOM are negatively associated with water clarity but positively associated with nutrients (Solomon et al. 2015; Isles et al. 2021; Sherbo et al. 2023). Some studies show that the opposing effects of these drivers of primary production lead to a unimodal response of phytoplankton productivity to DOM (Solomon et al. 2015; Kelly et al. 2018; Isles et al. 2021), while others demonstrate more consistent declines in primary productivity and food web productivity (Jackson and Hecky 1980; Carpenter et al. 1998; Karlsson et al. 2009; Hessen et al. 2017). For example, Karlsson et al. (2009) demonstrated how declines in light availability associated with DOM drove declines in whole lake primary production and fish productivity in boreal Swedish lakes by >75% (from their Fig. 2) even though total phosphorus (TP) increased. Similar results were found in our study region within the boreal region of Canada, where spatial (i.e., among-lake) increases of DOM from 2.5 to 9.5 mg DOC L^{-1} drove c. 70% declines in the biomass and productivity of phytoplankton, zoobenthos, zooplankton, and fish (Tonin et al. 2022; Sherbo et al. 2023; Tonin et al. 2025). While these studies provide strong support for the nutrient-colour paradigm, demonstrating how among-lake variations in lake DOM strongly influence a wide range of ecosystem properties at regional and larger spatial scales, the extent to which they represent temporal (i.e., within lake) ecosystem responses has been challenged (Stetler et al. 2021). Further, potentially important methodological differences among studies relate to the metric used to estimate phytoplankton biomass (e.g., chlorophyll *a* (Chl) or biovolume-based estimates) and how they are reported (e.g., epilimnetic concentrations or depth-integrated values). While many studies have evaluated the response of phytoplankton to DOM using epilimnetic Chl concentrations, the appropriateness of this indicator is questionable due to (a) failure to account for changes in sub-epilimnetic biomass that may account for a substantial fraction of depth-integrated biomass, (b) failure to account for variations in thermocline and photic depths that often co-occur with changes in DOM, and (c) failure to account for photoadaptation (or shifts in community structure) that may alter pigment concentrations without concomitant changes in biomass (Sherbo et al. 2023).

A growing number of studies have reported positive temporal trends of DOM within European lakes and those of eastern and central North America over the past several decades (Monteith et al. 2007; Weyhenmeyer et al. 2016; de Wit et al. 2021). For example, a recent survey of the temporal trends in DOM within 426 lakes in these regions showed that, between the years 1990 and 2016, DOM in the eastern North American lakes increased by c. 0.4 mg DOC L^{-1} $decade^{-1}$, with many European lakes showing increases >1.5 mg DOC L^{-1} $decade^{-1}$ (de Wit et al. 2021). The drivers of such increases appear twofold: the watersheds of many European lakes and those of northeastern North America were strongly affected by acid rain and as these watershed soils have recovered their binding affinity for organic carbon has declined; in addition, some of these regions have also experienced long-term increases in precipitation and air temperature that have led to increased runoff and DOM loading (Monteith et al. 2007, 2023; Meyer-Jacob et al. 2019; de Wit et al. 2021). At least two recent studies argue that climatic factors (i.e., precipitation, air temperature) are now equally or more important than factors associated with acid rain recovery for driving temporal changes lake DOM, including areas previously influenced by acid rain (Meyer-Jacob et al. 2019; de Wit et al. 2021).

The boreal forest ecozone includes between 30% and 60% of the world's lakes larger than 1 ha and represents a globally important carbon sink (Downing et al. 2006; Verpoorter et al. 2014; Heathcote et al. 2015). The Intergovernmental Panel on Climate Change (IPCC) reports a general positive trend of precipitation in boreal regions over the past several decades and projects continued increases through the 21st century (IPCC 2023). If our understanding of DOM effects derived from among-lake studies (i.e., space-for-time substitutions) hold true, the ecological effects of temporal changes in rainfall and DOM loading to freshwater ecosystems within the vast boreal ecozone are likely to be significant and have already begun. Here, we evaluate this assumption using the long-term (multi-decadal) trends and interrelationships between precipitation, DOM loading, lake DOM, and key ecosystem responses within boreal lakes at the IISD Experimental Lakes Area (ELA). The ELA study area, located in central Canada, is situated outside of regions strongly influenced by acid rain (Meyer-Jacob et al. 2019) but has undergone long-term changes in precipitation. Since the early 1900s annual precipitation at the ELA has oscillated between wet and dry periods, each lasting c. 10–16 years (Parker et al. 2009; Diodato et al. 2016; Meyer-Jacob et al. 2019). However, the most recent wet period (1990 to present) has persisted for over 30 years, with annual precipitation around 100 mm higher than that in previous wet periods (Emmerton et al. 2019; Meyer-Jacob et al. 2019) suggesting a disruption of previous patterns and the maintenance of higher sustained precipitation. The main objectives of our study were to: (1) quantify the long-term trends in lake DOM and its relationship with meteorological drivers; (2) assess and quantify the strength of relationships between lake DOM and key ecosystem properties; and (3) evaluate whether these temporal relationships between DOM and ecosystem properties are consistent with knowledge garnered from space-for-time substitutions.

Methods

Study area

The ELA resides in the Boreal ecozone and—with the exception of the research facility—the watersheds in the study area have remained entirely forested with negligible human development. The watersheds overlay Canada's Precambrian shield, with thin soils and primarily forested with jack pine (*Pinus banksiana*), red pine (*Pinus resinosa*), black spruce (*Picea mariana*), and white birch (Emmerton et al. 2019). The lakes are typically ice-covered from mid-November to late April (Higgins et al. 2021). The catchment of Lake 239 (L239) was partially burned in 1974 and so extensively in 1980 that soils in the upland portions of the catchment were burnt away exposing extensive bedrock (Bayley et al. 1992; Emmerton et al. 2019); the other catchments have not burned extensively within the last half century or longer. The effects of regional fires and reduced precipitation during earlier periods on DOM and ecosystem responses have been reviewed elsewhere (Schindler et al. 1996). While all of the study lakes have lake trout as the top predator, as well as minnow communities in the littoral zones and sculpin in profundal habitats, Lake 239 (L239) was the only study lake with planktivorous fish (e.g., *Coregonus artedii*) in pelagic habitats (Slongo et al. 2022).

Meteorology and hydrology

The ELA has co-operated a year-round meteorological station since 1968 with Environment and Climate Change Canada. Daily measurements of air temperature, precipitation (rainfall, snowfall), and event-based analyses of precipitation chemistry were collected. For one of the long-term ecological research (LTER) lakes (L239), water discharge within the inflow streams draining three sub-watersheds was measured continuously during the period of flow (April–November). Stream chemistry was measured weekly from May to October. While the monitoring program is ongoing, data analysis was restricted to the period prior to 2020 due

Table 1. Morphometric characteristics, locations, and study period for one polymictic lake (L114) and three dimictic (L224, L239, and L373) long-term reference lakes at the IISD Experimental Lakes Area used in the present study.

Parameter	Lake names L224	L239	L373
A_w (km^2)	0.975	3.39	0.829
A_0 (km^2)	0.259	0.543	0.273
V_L (m^3)	3066 671	6169 179	3107 474
Z_{mean} (m)	11.7	11.4	11.4
Z_{max} (m)	27.3	31.5	21.2
Mixing status	Dimictic	Dimictic	Dimictic
Latitude	49.6901	49.6627	49.7449
Longitude	−93.7169	−93.7227	−93.7987
Study period (years)	1974–2019	1969–2019	1987–2019

Notes: Watershed area (A_w), lake area (A_0), lake volume (V_L), mean lake depth (Z_{mean}), maximum lake depth (Z_{max}), and duration of monitoring record used within the present study (study period). Latitude and longitude represent locations of sampling location of each lake where depth is maximal. Lake metadata, except mixing status, study period, and watershed area are from IISD Experimental Lakes Area (ELA, 2022).

to reduced sampling frequency during 2020 and 2021 associated with the global coronavirus pandemic.

Nutrient loads to L239 were derived from three gauged inflow streams, unmeasured runoff, and direct precipitation on the lake surface. Total nutrient loads to L239 were determined using the methods of Hall et al. (2019). Daily loads from each of the three inflow streams were calculated using water discharge data and estimates of nutrient concentrations determined from linear interpolations between weekly collected chemistry data. Inputs from ungauged regions (approximately 30% of the watershed) were estimated by scaling the nutrient loads from the gauged watersheds on a per-area basis and assuming a 50:50 mix of inflows from the East and Northwest sub-basin streams (Hall et al. 2019). Precipitation loads were obtained using precipitation volumes to the lake surface and nutrient concentrations measured in precipitation.

Limnology

Physical, chemical, and biological properties of three dimictic, oligotrophic long-term reference lakes (Table 1; L224, L239, L373) were collected over varying lengths of time with the shortest dataset spanning 22 years (L373; 1982–2019). In addition to these nonmanipulated LTER lakes, a variety of other nonmanipulated dimictic lakes (>10 m in mean depth) were sampled intermittently over the 1970–2019 period; we refer to these lakes as the “regional lake dataset”. Sampling protocols were standardized across lakes and over time. Sampling for physical and chemical variables, and phytoplankton taxonomy occurred at the deepest part of each lake, typically on a biweekly (i.e., every 2 weeks) basis through the ice-free season. Water temperatures were measured using an RBR XRX-620 multi-function probe after 2009. Before 2009, temperatures were measured with a Flett Research Mark II Thermistor. Thermocline depth (Z_{therm}) was determined using the temperature profile data and the R program *rLakeAnalyzer* in RStudio (version 2022.12.0). Photosynthetically active radiation (PAR) was measured using an LI-192 Underwater Quantum Sensor. The attenuation of PAR in the water column (K_d) was determined as the slope of the line regressing ln(% PAR) versus depth (Fee et al. 1996). The euphotic depth (Z_{eu}) was defined as the depth of 1% surface irradiance. The mean light intensity within the water column of each dimictic lake (I_{mean}) was calculated as per Karlsson et al. (2009). Unless otherwise stated, data for all lakes are presented as mean values over the June–August (JJA) periods of strong thermal stratification within the dimictic lakes.

In most years, integrated water samples were collected biweekly (May–November) from the epilimnion (surface to Z_{therm}) and an operationally defined metalimnion (Z_{therm} to Z_{eu}) using an integrated sampler (Shearer 1978). Integrated water samples were analyzed for a large range of analytes including DOC, total nitrogen (TN), TP, particulate carbon (PC), Chl (Havens et al. 2024), and phytoplankton taxonomy and biovolume (see below). DOC was used as a surrogate for DOM. As with physical variables, water chemistry data for all lakes are presented as mean values across the JJA period of each year, when the water column of the lakes were thermally stable. Depth-integrated estimates (mg m^{-2}) of TN, and TP were calculated by multiplying concentrations (mg m^{-3}) by the thickness (m) of the respective layer (epilimnion and metalimnion) and summing the two layers. Volume weighted DOC, TN, and TP concentrations (mg m^{-3}) across the euphotic zone were calculated in a similar fashion but then divided by Z_{eu} (m). Depth-integrated Chl was calculated in two ways: (a) uncorrected for potential changes in Chl:PC with depth or over time (Chl$_{areal}$), and (b) corrected values (Chl$_{areal\_corr}$). Chl$_{areal}$ (mg m^{-2}) was calculated by multiplying mean layer specific Chl (mg m^{-3}) by the depth (m) of each layer (epilimnion, metalimnion) and then summing the two layers. For Chl$_{areal\_corr}$ prior to depth-integration, corrected Chl (Chl$_{corr}$) were calculated for each lake by multiplying annual mean PC by the mean Chl:PC ratio across all years (to account for the full range of water clarity) within each depth layer (epilimnion, metalimnion) of individual lakes. Values of Chl$_{corr}$ were then depth-integrated for each layer, and the areal values for the two layers were then summed. Changes in analytical instrumentation for any given parameter were always accompanied by cross calibration of samples before and after any changes were implemented. Additionally, the ELA analytical services lab participates in ongoing inter-lab proficiency testing as part of quality assurance/quality control protocols to ensure consistency over the long-term dataset. Detailed analytical and quality assurance/quality control protocols are provided elsewhere (Havens et al. 2024).

Phytoplankton taxonomy and biomass estimates of integrated epilimnetic and metalimnetic samples for each lake were undertaken by the same taxonomist over the complete timeseries using methods described elsewhere (Findlay et al. 2001). Subsamples (125 mL) of epilimnetic and metalimnetic water were preserved in Lugol’s solution until analysis. A 2 mL aliquot of the subsample was gravity settled for 24 h and species identification and enumeration were undertaken at 125X and 550X using the Utermöhl method (Nauwerk 1963). Cell measurements were undertaken to a maximum of 50 individuals within each species and cell numbers were converted to wet weight biomass by fitting shapes to geometric formulae assuming a specific gravity of 1.0 (Vollenweider 1968). Depth-integrated phytoplankton biomass within each layer (i.e., epilimnion, metalimnion) was calculated by multiplying biovolume-based phytoplankton biomass concentration (i.e., mg m^{-3}) by layer depth (i.e., m). Total depth-integrated phytoplankton biomass (B_{phyto}, mg m^{-2}) within each lake was calculated by summing values from the two layers on each sampling date, and seasonal averages through the period of stable thermal stratification were then calculated. While phytoplankton taxonomy samples from the epilimnion were collected from the start of each lake's timeseries, samples from the metalimnion were not routinely collected until 1980. Thus, depth-integrated biomass estimates could only be routinely calculated from 1980 onward.

Zooplankton samples were collected in L224 and L239 using two vertical hauls of a double-barreled 53 μm net from just above the lake bottom to the surface at the deep station (Chang and Malley 1987). Zooplankton in L373 were collected using a weighted flexible 7.6 cm diameter PVC hose that was lowered to just above the lake bottom and raised to the surface at six stations located at different depths and samples from different stations were combined before counting (Salki 1993). For L373 a 72 μm sieve was used prior to 1998 and a 53 μm one thereafter. Comparisons of counts made from samples sieved with the 53 and 72 μm nets indicated that Crustacea were sampled with equal efficiency (Johannsson et al. 1992). All samples were preserved with 4% sugar-formalin and crustacean zooplankton were counted until at least 300 animals had been identified to the lowest possible taxonomic category and life stage, with the exception that c4–c5 copepods were identified to species only after 1998.

Zooplankton population densities (individuals m^{-2} of lake surface area) were obtained by multiplying numbers per m^3 by maximum water depth in Lakes 224 and 239, which were sampled at the deep station only, or by mean depth in L373, which were sampled at multiple stations. Because zooplankton data from Lakes 239 and 224 are for the deep station and data from Lake 373 was derived from multiple stations, they are not directly comparable. Within each lake, however, trends over time are meaningful because consistent methods were used throughout. The biomass of each species and life stage (mg dry mass m^{-2}) was determined by multiplying population density (individuals m^{-2}) by mean individual biomass (mg dry mass individual^{-1}) estimated from length–weight regressions (Malley et al. 1989). Total zooplankton biomass was then obtained by summing the species and life-stage data.

Data analyses

The timeseries data were analysed over several different periods. The complete timeseries for each lake was used to assess relationships between precipitation, DOM loads, chemical and physical variables. Given the increasing availability and consistency of data collection for biotic variables within the study lakes from the 1980s onward, and that the 1980–2019 period represented a long-term increase in precipitation and DOM (see below), this period was chosen to assess the implications of increasing precipitation on DOM and limnological variables. Unidirectional trends over time were examined using Mann–Kendall trend tests and Sens slopes using the R (version 4.4.1) packages "Kendall" and "Trend"(McLeod 2022; Pohlert 2023).

Breakpoint analyses on timeseries data were undertaken using the R package "strucchange" (Zeileis et al. 2003), to identify significant structural changes in the annualized precipitation timeseries. The analysis considered models with varying number of breakpoints (0–5) and evaluated them based on residual sum of squares (RSS) and Bayesian information criterion (BIC). The breakpoint analysis identified a single breakpoint (see the "Results" section) around 1990 that, similar to Findlay et al. (2001), allowed an assessment of effects to limnological parameters during dry (1980–89) and wet (1990–2019) periods. Potential differences among decades were evaluated using mixed-effects models, with decade as the fixed effect and lake as the random effect, and Tukey post hoc tests from the R packages lme4 (Bates et al. 2015), emmeans (Lenth 2024), and multcomp (Hothorn et al. 2008). Normality was assessed visually from Q–Q plots.

To evaluate the relationship between phytoplankton biomass, Chl, DOM, and other potential drivers (e.g., nutrients, light) across multiple lakes, we used a linear mixed-effects model (LMM) with the package lme4 in R (Bates et al. 2015). Chl, DOM, and other potential drivers included as a fixed effect within the models, while lake was modeled as a random intercept to account for among lake variation in phytoplankton biomass. In all cases where heteroscedasticity was apparent, values were log transformed prior to analysis.

Results

Long-term changes in meteorology and chemical loads

Between 1969 and 2019, mean annual air temperatures at the ELA increased by c. 1.5 °C (Fig. S1; see also (Guzzo and Blanchfield 2017)). The largest changes occurred in the winter months (December–February) when the lake surfaces were frozen (Fig. S1). Air temperatures did not change significantly in spring, summer, or autumn (March–November, Fig. S1), although increasing autumn temperature trends (+0.3 °C decade^{-1}) approached the level of significance ($p = 0.07$). Annual precipitation in the study region ranged from 488 to 1018 mm year^{-1} ($n = 51$, 727 ± 139 mm, Fig. 1). For the period (1980–2019) that spanned the most recent dry–wet portion of the precipitation cycle (Emmerton et al. 2019), a significant upward trend in total precipitation ($n = 40$, $\tau = 0.30$, $p = 0.007$) was detected, with a Sen's slope of 5.3 mm year^{-1} (95% CI: 1.5–9.2 mm year^{-1}; Fig. 1). The upward trend in total precipitation was primarily driven by an upward trend in annual rainfall ($\tau = 0.23$, $p = 0.036$), with a Sen's slope of 3.7 mm year^{-1} (95% CI: 0.2–7.2 mm year^{-1}). The long-term (1980–2019) monotonic trend in snowfall was positive ($\tau = 0.23$, $p = 0.037$), but it increased at a slower rate (Sen's slope of 1.3 mm year^{-1}; CI: 0.11–2.6 mm year^{-1}). Our analysis using mixed-effects modelling also indicated a significant increase

Fig. 1. Long-term (1970–2019) changes in annual precipitation (thin solid line) at the IISD Experimental Lakes Area meteorological station, located within the L239 watershed. The thick dark line and shaded area represent the loess fit and the 95% confidence interval, respectively. The vertical dashed line represents the delineation between the most recent dry (1980–2019) and wet (1990–2019) periods as determined by breakpoint analysis.

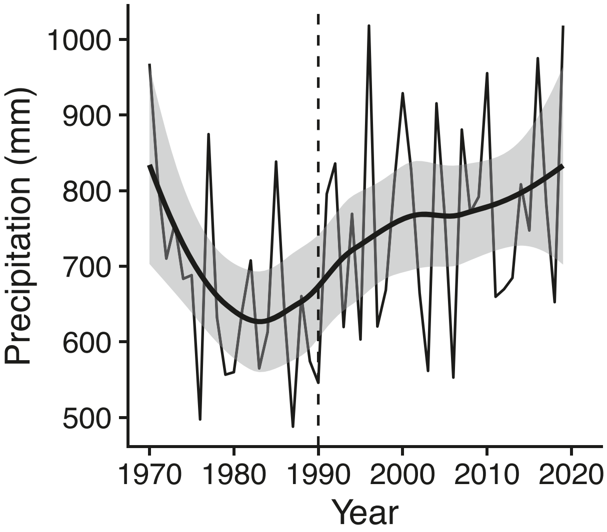

in decadal precipitation between the 1980–1989 period and the 2000–2009 and 2010–2019 periods, while 1990–1999 represented a period of transition between the two states (Table 2). Consistent with this finding, breakpoint analyses revealed a structural change in annual rainfall data around the year 1990, marking a delineation between the most recent dry (1980–1989) and wet (1990–2019) periods. The model containing the single breakpoint represented a substantial improvement in model fit (RSS: 571052, BIC: 636.0) compared with to the null model with no breakpoints (RSS: 698779, BIC: 638.4). No significant structural changes in the snowfall or total precipitation over the full (1970–2019) timeseries were detected. However, the winter of 1970 contained the highest snowfall within the 50-year record (Fig. S2), which contributed to very high total precipitation for that year (Fig. 1). When the breakpoint analysis was performed on the 1971–2019 period for snowfall, there remained no significant structural changes in the timeseries, but structural changes in total annual precipitation timeseries were detected at the year 1990 resulting in a substantial improvement in model fit (RSS: 678614, BIC: 633.3) compared to the null model with no breakpoints (RSS: 824633, BIC: 635.3). Increases in precipitation after the 1990 breakpoint (Fig. 1; Table 2) were not statistically significant as indicated by both the Mann–Kendall trend test ($n = 30$, $\tau = 0.15$, $p = 0.25$) and the mixed-effects model (Table 2).

Annual DOM loading from the intensively monitored L239 watershed displayed a strong linear relationship with annual precipitation ($n = 48$, $R^2 = 0.77$, $p < 0.0001$; Fig. 2*a*). As precipitation increased over the past 40 years (1980–2019), DOM trended upwards (Fig. 3*a*) within the three dimictic lakes (L224, L239, and L373). DOM in L239 increased most rapidly; the upward DOM trend for L239 ($n = 40$, $\tau = 0.38$, $p < 0.001$) had a Sen's slope of 0.03 mg L^{-1} year^{-1} (95% CI: 0.02–0.05 mg L^{-1} year^{-1}); for L224 the upward DOC trend ($n = 36$, $\tau = 0.57$, $p < 0.0001$) had a Sen's slope of 0.02 mg L^{-1} year^{-1} (95% CI: 0.01–0.03 mg L^{-1} year^{-1}); and for L373 the upward DOC trend ($n = 34$, $\tau = 0.25$, $p = 0.038$) had a Sen's slope of 0.01 mg L^{-1} year^{-1} (95% CI: 0.001–0.017 mg L^{-1} year^{-1}). Our mixed-effects modelling indicated that the 1990s was period of transition; it was not until the 2000s that epilimnetic DOM concentrations became significantly different from the low precipitation conditions of the 1980s, and concentrations during the 2010s remained high and not significantly different from the previous decade (Table 2). However, volume-weighted DOM concentrations across the euphotic zone during the 1990–1999 period showed a significant increase from the 1980 to 1989 period and increased during the 2010–2019 period (Table 2). Nutrient loads (TN, TP) from the L239 watershed were also positively correlated with precipitation (Figs. 2*b* and 2*c*).

Physical and chemical properties

Lake DOM concentrations were strongly linked to the physical properties within the three study lakes and among other regional dimictic lakes (Fig. 4). DOM altered several metrics associated with light availability. The relationship between DOC and K_d within the study lakes was consistent with the regional lake dataset, which was positive and approximately linear between c. 2.5 and 10 mg DOC L^{-1} (Fig. 4*a*). Values of K_d, averaged across the three dimictic study lakes, increased by c. 0.1 m^{-1} between the 1980s and subsequent decades (Table 2). Estimates of I_{mean} (mean irradiance within lake) and Z_{eu} (depth of the euphotic zone), which are derived from K_d but incorporate the logarithmic relationship between K_d and light transmission, were also strongly influenced by DOM (Figs. 4*b*–4*d*). Both I_{mean} and Z_{eu} declined by c. 20%–23% in each of our three dimictic lakes over the study period (Fig. 3*b*; Table 2). From the 1980–1989 period to the 2010–2019 period, Z_{eu} declined from 19.0 ± 1.5 to 14.1 ± 1.0 m in L224, from 7.8 ± 1.0 to 6.5 ± 0.7 m in L239, and from 15.2 ± 1.2 to 11.1 ± 0.8 m in L373. As a result of the changes in Z_{eu}, the proportion of lake volume (V_{eu}) above Z_{eu} within the study lakes also declined from c. 77% to c. 67% of total lake volume over the study period (Table 2). Within our study lakes Z_{therm} declined (i.e., became shallower) by c. 17% between the 1980 and 1989 "drought" period and subsequent decades (Fig. 3*c*; Table 2) and there was a significant relationship between DOM and Z_{therm} within the regional lake dataset (Fig. 4*d*). From the 1980–1989 period to the 2010–2019 period, Z_{therm} declined from 9.1 ± 0.7 to 7.4 ± 0.7 m in L224, from 7.2 ± 0.5 to 5.7 ± 0.4 m in L239 and from 7.6 ± 1.1 to 6.7 ± 0.8 m in L373 (Fig. 3*c*).

Decadal mean values of volume-weighted TP within the euphotic zone ranged from c. 5.1 to 6.5 mg m^{-3}, and decadal mean values of volume-weighted TN within the euphotic zone ranged from 255 to 295 mg m^{-3} within the dimictic study lakes across the 1980–2019 study period (Table 2)

Table 2. Decadal parameter values (mean ± SD) for meteorological and lake data.

Variable	1980–1989	1990–1999	2000–2009	2010–2019
Meteorological				
Precipitation (mm)	631 ± 95^{a}	729 ± 138^{b}	766 ± 130^{b}	795 ± 135^{b}
Physical				
K_d (m^{-1})	0.39 ± 0.17^{a}	0.42 ± 0.15^{b}	0.47 ± 0.18^{c}	0.48 ± 0.17^{c}
I_{mean}	0.25 ± 0.8^{a}	0.23 ± 0.06^{b}	0.21 ± 0.06^{c}	0.20 ± 0.06^{c}
Z_{eu} (m)	13.7 ± 5.1^{a}	12.2 ± 3.6^{b}	11.0 ± 3.6^{c}	10.6 ± 3.3^{c}
V_{eu} (%)	76.8 ± 21.3^{a}	73.2 ± 17.6^{b}	68.2 ± 18.2^{c}	66.7 ± 17.3^{c}
Z_{therm} (m)	8.0 ± 1.1^{a}	7.2 ± 1.1^{b}	7.2 ± 1.0^{b}	6.6 ± 0.9^{c}
Chemical				
DOC_{epi} (g m^{-3})	4.7 ± 1.7^{a}	4.7 ± 1.5^{a}	5.0 ± 1.6^{b}	5.1 ± 1.7^{b}
DOC_{photic} (g m^{-3})	4.9 ± 1.9^{a}	4.8 ± 1.9^{a}	5.6 ± 2.0^{b}	5.5 ± 2.1^{b}
TP_{epi} (mg m^{-3})	6.4 ± 1.7^{a}	5.1 ± 0.7^{b}	6.2 ± 1.2^{a}	6.3 ± 1.1^{a}
TP_{photic} (mg m^{-3})	6.3 ± 2.3^{a}	5.5 ± 0.9^{a}	6.3 ± 1.2^{a}	6.5 ± 1.3^{a}
TN_{epi} (mg m^{-3})	264 ± 45^{a}	242 ± 35^{b}	284 ± 42^{c}	259 ± 41^{a}
TN_{photic} (mg $^{-3}$)	270 ± 45.5^{a}	255 ± 40.8^{a}	299 ± 53.9^{b}	267 ± 44.3^{a}
Biological				
Chl_{epi} (mg m^{-3})	1.5 ± 0.7^{a}	1.8 ± $0.7^{a,b}$	2.0 ± 0.6^{b}	1.9 ± 0.7^{b}
Chl_{epi}:B_{phyto}	0.24 ± 0.17^{a}	0.45 ± 0.38^{b}	0.56 ± 0.36^{b}	0.42 ± 0.23^{b}
Chl_{areal_corr} (mg m^{-2})	22.0 ± 6.7^{a}	22.5 ± 5.5^{a}	21.1 ± 5.1^{a}	18.4 ± 5.1^{b}
B_{phyto_epi} (mg m^{-3})	510 ± 144	346 ± 108^{b}	356 ± 140^{b}	402 ± 144^{b}
B_{phyto} (mg m^{-2})	1717 ± 541^{a}	1115 ± 355^{b}	1060 ± 425^{b}	1170 ± 423^{b}
B_{zoop} (mg m^{-2})	11.0 ± 3.6^{a}	9.5 ± 4.9^{a}	11.9 ± 4.9^{a}	10.1 ± 3.9^{a}

Note: DOC and nutrient concentration were reported as concentrations within the epilimnion (e.g., DOC_{epi}) and volume-weighted concentrations across the euphotic zone (e.g., DOC_{photic}). Chlorophyll *a* was reported as epilimnetic concentrations (Chl_{epi}) and depth-integrated values across the euphotic zone that were corrected for photo-adaptation ($Chl_{areal\_corr.}$). Reported values of Chl_{epi}:B_{phyto} were multiplied by 1000 for display purposes. Depth-integrated crustacean zooplankton biomass (B_{zoop}) represents only L239 due to insufficient data for other reference lakes during the 1980–1989 reference period. Superscripts represent of Tukey post hoc test results, with corresponding colours representing a significant increase (green) or decrease (red) from the 1980 to 1989 period. Significant differences among decades were assessed using mixed-effects models and Tukey's post hoc test. The analysis was undertaken on the meteorological data and limnological data from the three dimictic study lakes (L224, L239, and L373) at the IISD Experimental Lake Area, Canada. DOC, dissolved organic carbon; TP, total phosphorus; TN, total nitrogen. Superscripts represent Tukey post-hoc test results with different letters indicating a significant difference between periods.

and were similar to epilimnetic concentrations. Despite the upward trend in precipitation over the study period and the strong correlation between precipitation and nutrient loads, and between DOM and volume-weighted TN ($n = 137$, $R^2 = 0.68$, $p < 0.0001$) and TP ($n = 137$, $R^2 = 0.07$, $p = 0.0013$) (Fig. 5), we did not observe a consistent temporal trend in nutrient concentrations within lakes (Fig. 3*d*) as assessed by the Mann–Kendall trend test over the 1980–2019 study period (except TP within L373, which showed a significantly positive trend ($n = 37$, $\tau = 0.28$, $p = 0.022$)). Decadal assessments of nutrient concentrations using mixed-effects models showed a similar result, with no consistent trend in nutrient concentrations over the 1980–2019 period (Table 2). In part, this response may have reflected high nutrient concentrations (e.g., Fig. 3*e*) during the early 1980s that were carried over from previous wet periods. Following the breakpoint in 1990, TP trended upwards in the three dimictic lakes (L224: $n = 30$, $\tau = 0.29$, $p = 0.03$ with a Sen's slope of 0.04 mg m^{-3} $year^{-1}$; L373: $n = 30$, $\tau = 0.29$, $p = 0.03$ with a Sen's slope of 0.06 mg m^{-3} $year^{-1}$; L239: $n = 30$, $\tau = 0.37$, $p = 0.004$ with a Sen's slope of 0.07 mg m^{-3} $year^{-1}$). An upward trend in epilimnetic TN only occurred in L239 ($n = 30$, $\tau = 0.29$, $p = 0.03$) with a Sen's slope of 1.04 mg m^{-3} $year^{-1}$.

Biota

Epilimnetic Chl concentrations within the study lakes increased by c. 27% over the study period (Table 2) and there were a positive linear relationships between epilimnetic DOC or K_d versus Chl within the study lakes and regional lakes (Fig. S3*a*). However, the Chl:B_{phyto} ratio within the epilimnion increased by >60% between 1980 and 1989 and subsequent decades (Table 2) and both Chl:B_{phyto} and Chl:PC were positively correlated with epilimnetic DOM and K_d (Figs. S3b–c, S4b–c) suggesting photoadaptation (or community level shifts) may have occurred in response to reduced water clarity. In contrast, epilimnetic phytoplankton biomass (as biovolume) when reported as volumetric units (i.e., mg m^{-3}) declined within the study lakes (Table 2) and there was no significant relationship ($p = 0.25$) between epilimnetic Chl and B_{phyto} (Fig. S5; Table S1) as detected by the LMM for both the study lakes and regional lakes. While epilimnetic Chl was a poor predictor of depth-integrated phytoplankton biomass within the euphotic zone (B_{phyto}), we also investigated relationships between B_{phyto} and depth-integrated chlorophyll *a* that were corrected (Chl_{areal_corr}) and uncorrected (Chl_{areal}) for photoadaptation using Chl:PC ratios (see the "Methods" section). The LMM indicated no significant relationship between

Fig. 2. The linear relationship between annual precipitation and whole watershed loads of: (*a*) dissolved organic carbon (DOC, $y = 54x - 21\,743$, $n = 48$, $R^2 = 0.77$, $p < 0.0001$), (*b*) total nitrogen (TN, $y = 1.6x - 328$, $n = 49$, $R^2 = 0.68$, $p < 0.0001$), (*c*) and total phosphorus (TP, $y = 0.05x - 12$, $n = 49$, $R^2 = 0.45$, $p < 0.0001$) from the L239 watershed at the IISD Experimental Lakes Area.

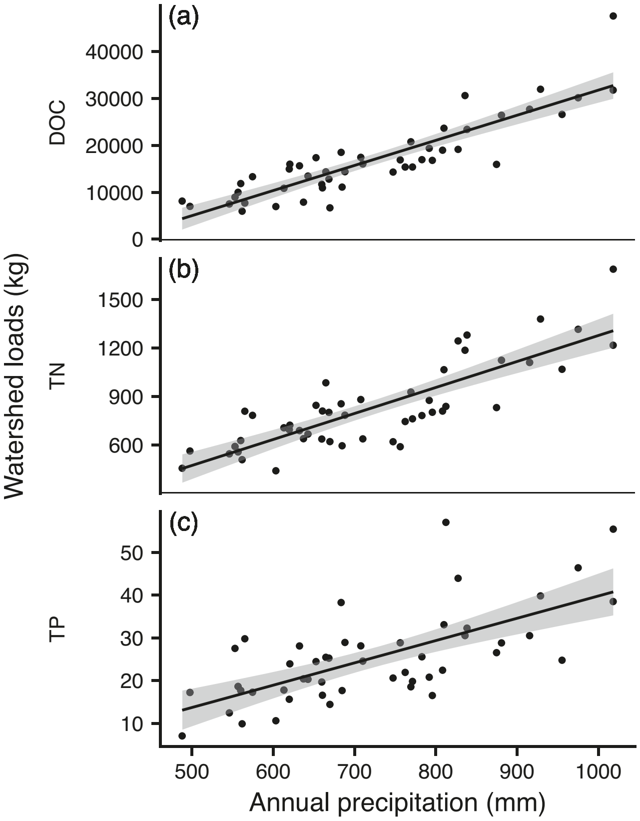

Chl_{areal} and B_{phyto} ($p = 0.89$). However, the LMM indicated that the fixed effect of Chl_{areal_corr} for predicting B_{phyto} was positive and highly significant (Fig. 6, $p < 0.0001$), indicating that once corrections for photoadaptation were incorporated within estimates of depth-integrated Chl (i.e., Chl_{areal_corr}) it was a potentially useful indicator of B_{phyto}.

We evaluated the response of depth-integrated phytoplankton indicators (B_{phyto} and Chl_{areal_corr}) to DOM in several ways. First, the LMM model and Tukey post hoc tests indicated that across our study lakes both B_{phyto} and Chl_{areal_corr} declined by 17%–38% over the same timeframe as precipitation and DOM increased, although Chl_{areal_corr} was somewhat less responsive than B_{phyto} (Table 2). Second, the LMM indicated that both B_{phyto} and Chl_{areal_corr} displayed significant negative relationships with DOM across the study lakes and regional lakes (Figs. 7*a* and 7*b*; Tables S1 and 2). Third, the LMM model indicated significant positive effects of I_{mean} on both B_{phyto} and Chl_{areal_corr} (Figs. 8*a* and 8*b*; Tables S1 and S2). Fourth, we found no significant relationships ($p > 0.05$, Tables S1 and S2) between indicators of phytoplankton biomass (B_{phyto} or Chl_{areal_corr}) and nutrient (TN, TP) concentrations that were volume-weighted across the euphotic zone. Finally, the LMM indicated positive relationships between I_{mean}:TP and both B_{phyto} (Fig. S6) and Chl_{areal_corr}, and a negative relationship between DOC:TP and Chl_{areal_corr} but no significant relationship between DOC:TP and B_{phyto} (Tables S1 and S2). As TP was uncorrelated with B_{phyto} (Fig. S7; Table S1) and Chl_{areal_corr} (Table S2), we interpreted that relationships between the indicators of phytoplankton biomass and the two ratios (DOC:TP and I_{mean}:TP) were primarily driven by variation of DOC or I_{mean}.

There was no significant relationship between B_{zoop} and DOC ($p > 0.05$) or significant temporal trends in B_{zoop} (Fig. 3*f*) within the dimictic study lakes over the 1980–2019 period as detected by either the Mann–Kendall trend tests ($p > 0.05$) or mixed-effects modelling (Table 2).

Discussion

In the boreal ecozone of central Canada, our long-term monitoring records indicated that DOM loads approximately doubled since the 1980s and that c. 80% of the variance in annual DOM loads was explained by precipitation alone, which is consistent with other studies over a shorter time period (Hall et al. 2019). While studies from northeastern North America and Europe have described the important effects of acid rain and soil acidity on DOM loading to lakes (Monteith et al. 2007; Meyer-Jacob et al. 2019), the strong relationship we found between precipitation and DOM loads was not surprising; while SO_4 deposition in the region has declined since the 1980s and significant (albeit weaker) relationships between SO_4 and lake DOM have been reported (Imtiazy et al. 2025), the ELA study area was outside the area in northeastern North America strongly influenced by acid deposition (Meyer-Jacob et al. 2019). Further, even within regions more strongly influenced by historical acid deposition, strong relationships between discharge and DOM loads have been reported (Erlandsson et al. 2008). Given the widespread historical and projected increases in precipitation across the boreal ecozone noted by the IPCC (IPCC 2023), if such causal relationships between precipitation and DOM loading hold true for other boreal regions (e.g., Weyhenmeyer et al. 2016), it is likely that a large proportion of the world's lakes, not only those in regions recovering from acid rain, are experiencing increased loads of allochthonous DOM and that such trends are likely to continue.

The increases in DOM within our study lakes since the 1980s (0.1–0.3 mg DOC L^{-1} $decade^{-1}$) were somewhat less than reported for eastern North America and Europe (c. 0.3–1.5 mg DOC L^{-1} $decade^{-1}$) over similar timeframes (Meyer-Jacob et al. 2019; de Wit et al. 2021). We speculate that the lower temporal trends in the ELA region result from the relatively thin soils overlaying the Precambrian shield, historical forest fires in the L239 catchment, the reduced historical effects of acidification relative to other sites, the lack of increase in summer air temperatures relative to other sites that would influence decomposition rates for terrestrial organic matter, or a combination of these factors. Compared with spatial variation (≥12 mg DOC L^{-1}) in DOM among regional lakes (Sherbo et al. 2023) the temporal increase of DOM within the study lakes over the c. 40-year study period were modest (0.4–1.2 mg DOC L^{-1}). Nonetheless, these temporal

Fig. 3. Long-term variation in (*a*) dissolved organic carbon (DOC), (*b*) mean water column irradiance (I_{mean}, proportion of surface irradiance), (*c*) thermocline depth (Z_{therm}), (*d*) total phosphorus (TP), (*e*) depth-integrated phytoplankton biomass (B_{phyto}), and (*f*) depth-integrated zooplankton biomass (B_{zoop}) for three dimictic lakes at the IISD Experimental Lakes Area. Average seasonal (June–August) values for each parameter are presented with loess fits (dark lines) and 95% confidence intervals (grey shaded areas). The vertical dashed lines represent the delineation between the most recent dry (1990–1989) and wet (1990–2019) periods as determined by breakpoint analysis. DOC and TP represent volume-weighted mean values across the euphotic zone.

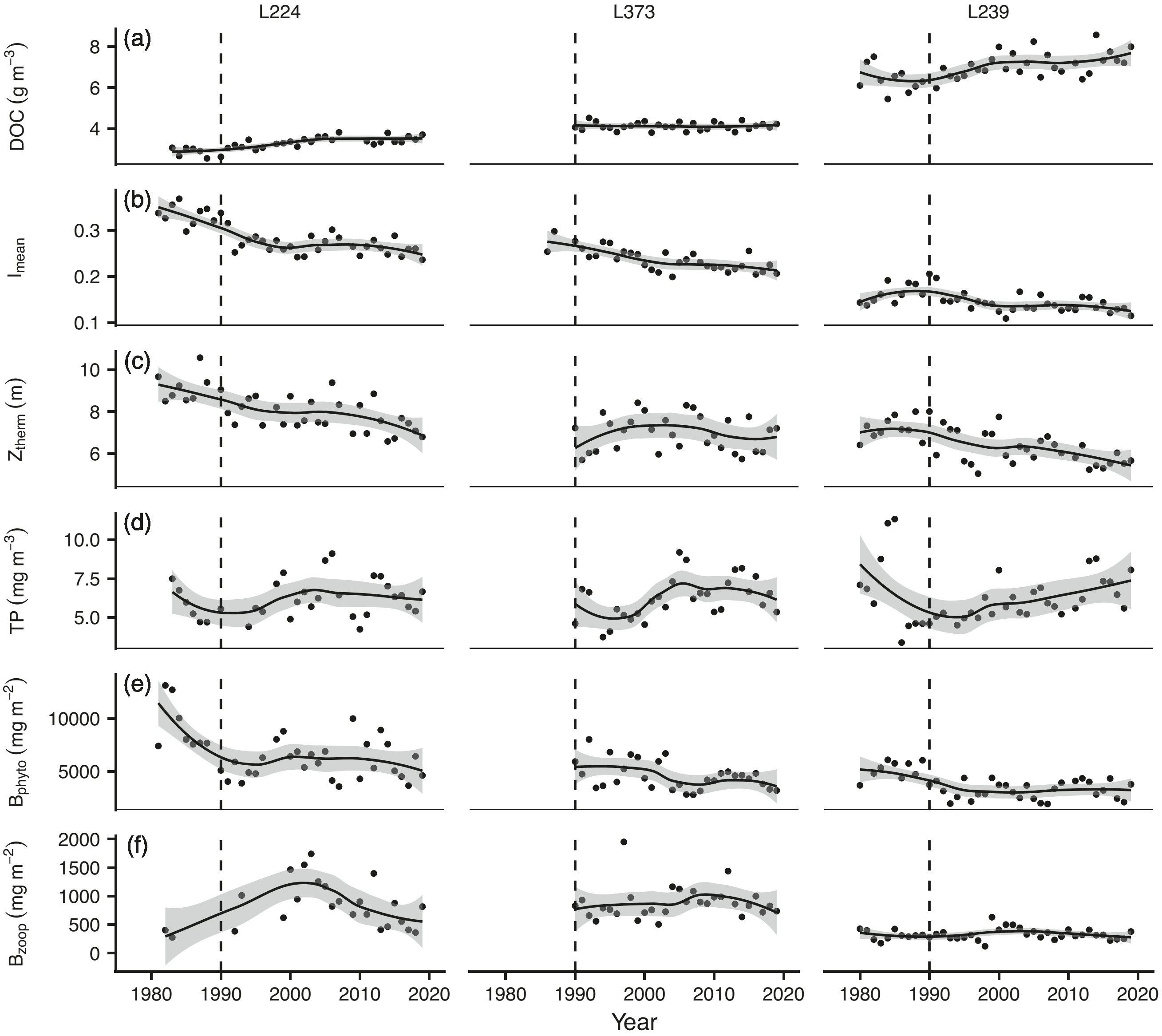

changes in lake DOM were associated with ecologically relevant changes to their limnological properties.

The nutrient-colour paradigm for lakes emphasizes the role of DOM in altering the optical properties of lakes, with cascading effects to a wide range of ecosystem processes and properties (Williamson et al. 1999; Karlsson et al. 2009). Across regional lakes, water clarity was tightly controlled by DOM; K_{d} was linearly correlated to DOM, with DOM explaining >80% of its variance. Across the 1980–2019 period where precipitation and DOM trended upwards, temporal increases in K_{d} within the study lakes appeared modest (Δ +0.07 to +0.11 m^{-1}), especially when comparing with spatial variation (>Δ 1.0 m^{-1}) among regional lakes. However, owing to the exponential nature of the Beer–Lambert Law, these temporal changes in K_{d} had large effects on the transmission of PAR through the water column. Mean availability of PAR across the dimictic lakes (I_{mean}) declined over the study period by c. 17%–25% and Z_{eu}, which is commonly used to estimate the maximum depth where plant growth occurs, declined by 17%–26%. As a result, the volume of the euphotic zone (V_{eu}) within the dimictic study lakes also declined by c. 14%–18%. Consistent with the nonlinear effects of DOM on Z_{eu} found among spatial studies (Jones 1992; Sherbo et al. 2023), the strongest effects were found in lakes with lower initial DOM

Fig. 4. Relationships between volume-weighted dissolved organic carbon (DOC) within the euphotic zone and the light attenuation coefficient (K_d, $y = 0.09x + 0.001$, $n = 157$, $R^2 = 0.88$, $p < 0.0001$), mean water column light intensity (I_{mean}, proportion of surface irradiance), $y = -0.019x + 0.33$, $n = 157$, $R^2 = 0.34$, $p < 0.0001$), euphotic depth (Z_{eu}, $y = 45.2 \cdot e^{-0.47x} + 5.63$, $n = 160$, $R^2 = 0.91$, and thermocline depth (Z_{therm}, $y = -0.45x + 9$, $n = 160$, $R^2 = 0.45$, $p < 0.0001$) within study lakes (blue = L224, red = L239, green = L373) and regional dimictic lakes (grey).

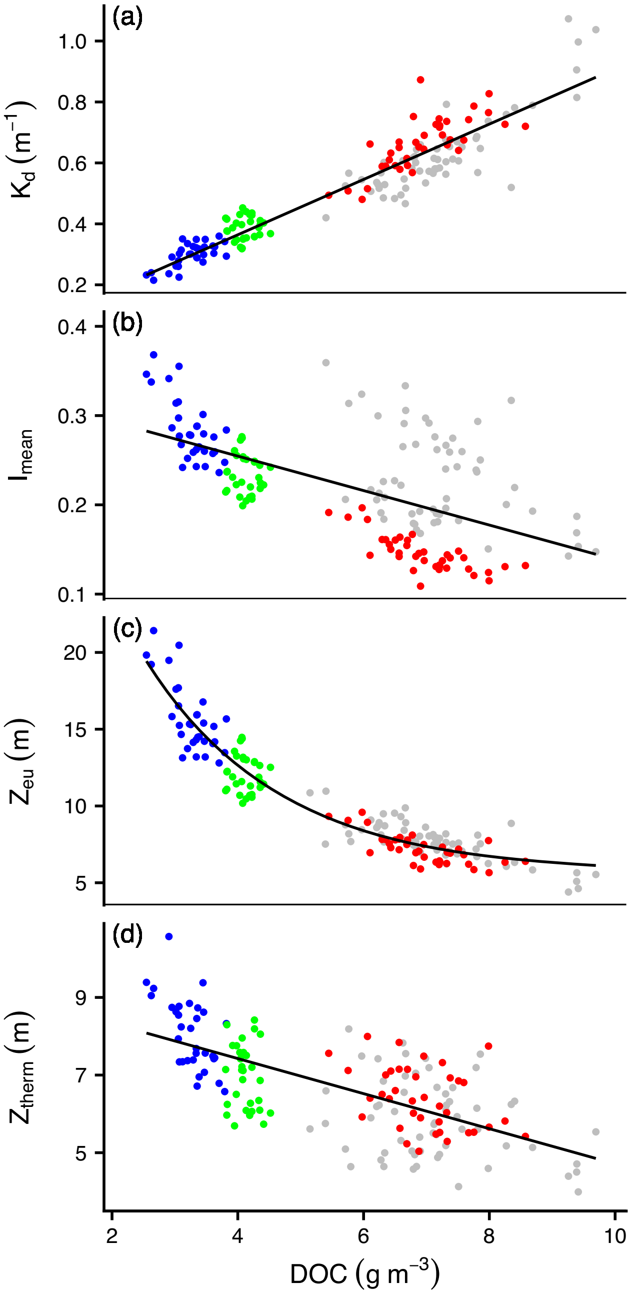

concentrations. These results indicate that even the modest temporal increases in DOM and K_d within the study lakes had ecologically significant effects on water column PAR and the availability of habitat to support primary production.

Fig. 5. Linear relationship between volume-weighted dissolved organic carbon (DOC), volume-weighted total nitrogen (TN, $y = 28x + 134$, $n = 134$, $R^2 = 0.68$, $p < 0.0001$), and volume-weighted total phosphorus (TP, $y = 0.27x + 5$, $n = 134$, $R^2 = 0.11$, $p < 0.0001$) within the euphotic zone of the study lakes (blue = L224, red = L239, green = L373) and regional dimictic lakes (grey).

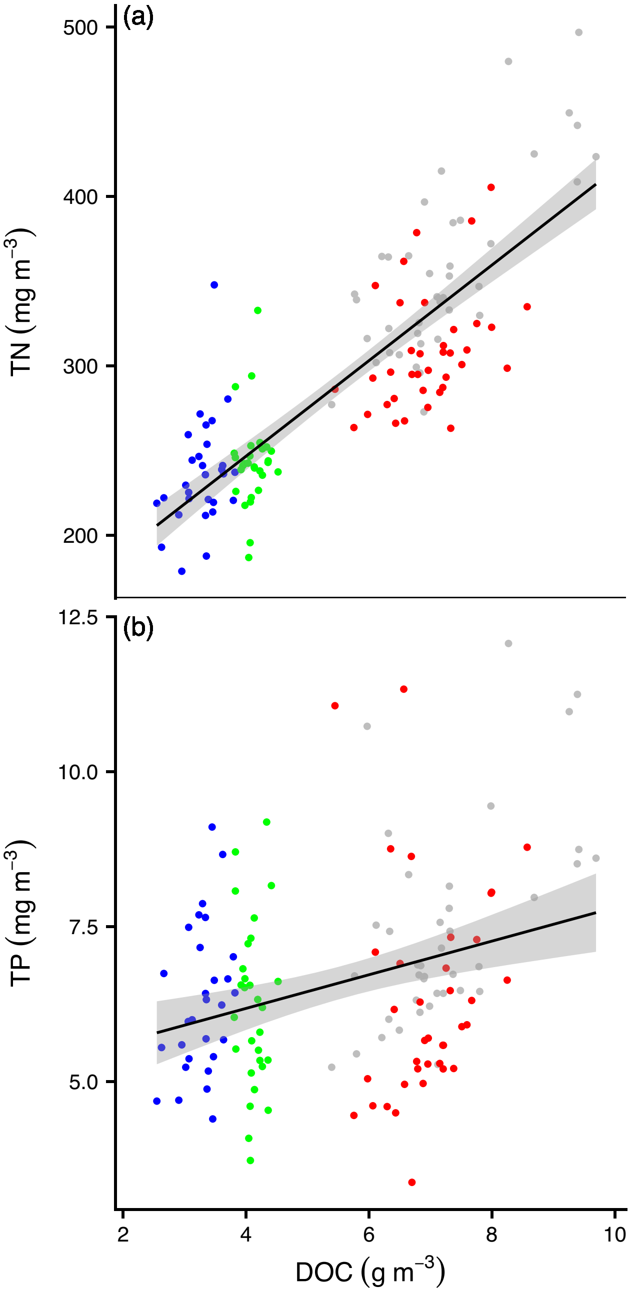

DOM and its effects on the optical and chemical (i.e., nutrients) properties of lakes strongly influence autotrophic productivity with the potential to cascade throughout lake food webs (Karlsson et al. 2009; Creed et al. 2018). Our results indicated that epilimnetic Chl concentrations, which are often used as indicators of phytoplankton biomass, were positively correlated with DOM and increased by c. 27% over the study period, concomitant with the increases in precipitation and

Fig. 6. Relationship between depth-integrated phytoplankton biomass (B_{phyto}) and depth-integrated chlorophyll *a* corrected for photoadaptation ($Chl_{areal\_corr.}$) within study lakes (blue = L224, red = L239, green = L373) and regional lakes (grey). A multi-level linear mixed model was used to assess the overall positive relationship ($p < 0.0001$) among lakes (see the "Results" section).

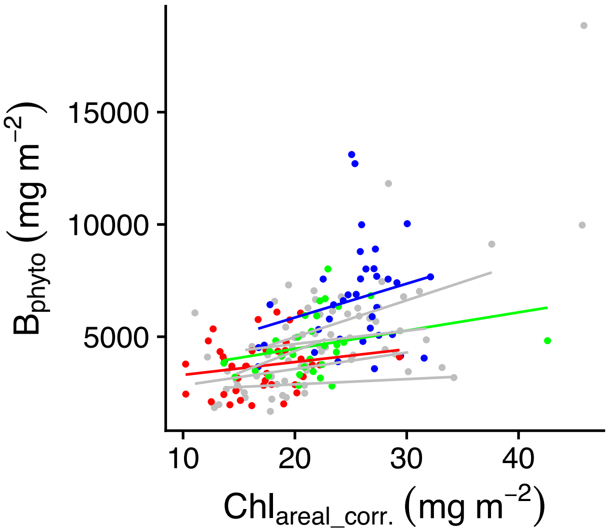

Fig. 7. Relationship between volume-weighted dissolved organic carbon (DOC) within the euphotic zone and (*a*) depth-integrated chlorophyll *a* corrected for photoadaptation ($Chl_{areal\_corr.}$) and (*b*) depth-integrated phytoplankton biomass (B_{phyto}) within study lakes (blue = L224, red = L239, green = L373) and regional dimictic lakes (grey). A multi-level linear mixed model was used to assess the overall negative relationship ($p < 0.0001$) among lakes (see the "Results" section).

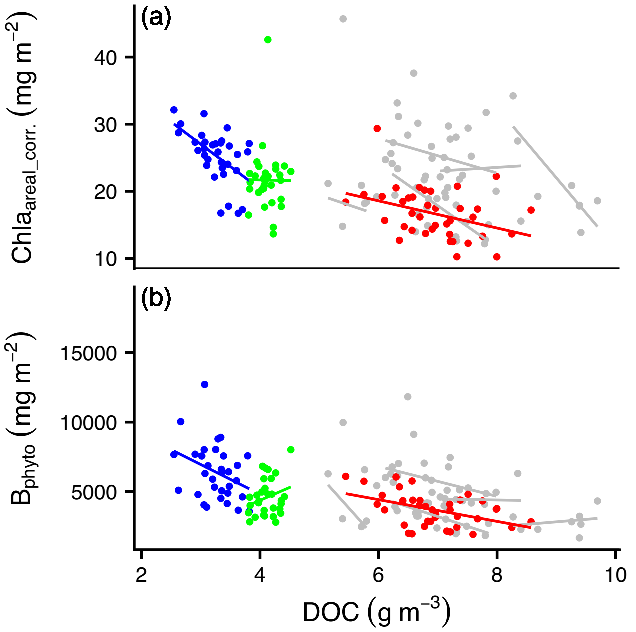

Fig. 8. Relationship between mean water column light intensity (I_{mean}) and depth-integrated phytoplankton biomass (B_{phyto}) within study lakes (blue = L224, red = L239, green = L373) and regional dimictic lakes (grey). A multi-level linear mixed model was used to assess the overall positive relationship ($p < 0.0001$) among lakes (see the "Results" section).

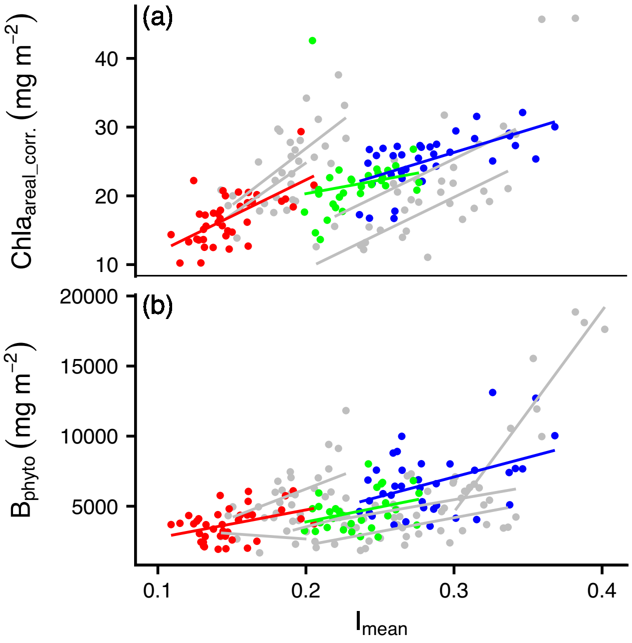

DOM. Other studies have also reported positive relationships between DOM and epilimnetic Chl concentration (Nurnberg and Shaw 1998; Webster et al. 2008; Isles et al. 2021), inferring a positive response of phytoplankton biomass to DOM in response to increased nutrients associated with DOM or potentially due to a concentrating of phytoplankton within a shrinking photic zone (Jones 1992). However, as noted by others (Kruskopf and Flynn 2006; Senar et al. 2021) and quantified by Sherbo et al. (2023), the use of algal pigments as indicators of phytoplankton biomass is complicated by the capacity of phytoplankton cells to alter their pigment content, or shift their community structure to species with higher Chl:Biomass ratios, in response to changing light conditions. Further, epilimnetic Chl concentration did not account for changes in sub-epilimnetic phytoplankton biomass nor variations in Z_{therm} and Z_{eu} that were driven by DOM. These effects represent a particular challenge for studies evaluating the response of phytoplankton across spatial or temporal gradients of DOM using epilimnetic Chl since DOM drove variations in water clarity, I_{mean}, Z_{therm}, Z_{eu}, and the ratio of Chl to phytoplankton biomass. Indeed, epilimnetic Chl within our study lakes was such a poor indicator of DOM's effects on depth-integrated phytoplankton biomass that it incorrectly estimated both the magnitude and direction of effect. However, we also assessed the utility of depth-integrated Chl as an indicator of the phytoplankton response to DOM and assessed whether corrections for photoadaptation were required. Our results indicated that depth-integrated Chl that was uncorrected for photoadaptation was a poor predictor of B_{phyto}. However, once corrections for photoadaptation had been made, depth-integrated Chl was a useful indicator of B_{phyto} and reasonably predicted the temporal response to increased precipitation and DOM.

The temporal response of depth-integrated phytoplankton biomass within the study lakes was consistent with an earlier space-for-time analysis within the same study region (Sherbo et al. 2023) that also demonstrated a strong negative effect of DOM. While the study lakes examined here were oligotrophic and strongly nutrient limited, depth-integrated phytoplankton biomass declined by 19%–25% over the study period even as precipitation, DOM, and nutrient loads increased. In a temporal study of previously acidified Adirondak lakes in the northeastern USA, increases in DOM were associated with declines in estimated phytoplankton photosynthesis within 17 of the 28 lakes examined, which was attributed to temporal reductions in both water clarity and nutrients (Stetler et al. 2021). In that study, the temporal responses of nutrients and the ratio of DOM:nutrients differed from analyses using space-for-time substitutions (Stetler et al. 2021). In our study, where temporal increases in precipitation—rather than recovery from acidification—drove increases in DOM and nutrients we also found consistent declines in depth-integrated phytoplankton biomass and the results were consistent with the regional space-for-time substitutions reported by Sherbo et al. (2023). The lack of a positive effect of nutrient enrichment on B_{phyto} in our oligotrophic study lakes was somewhat surprising given that whole-ecosystem nutrient (phosphorus or nitrogen + phosphorus) addition experiments conducted on nearby (<25 km) lakes led to large increases in phytoplankton productivity and biomass (Schindler and Fee 1974; Paterson et al. 2011; Molot et al. 2021), and concur with studies suggesting limited bioavailability of nutrients associated with DOM (Jackson and Hecky 1980; Francko 1986; Maranger and Pullin 2003). As with the study by Hessen et al. (2017) on boreal lakes in Scandinavia, it may also be that increased nutrient loads associated with DOM partially offset the reductions in phytoplankton growth and biomass resulting from higher light attenuation, but the negative effects of DOM on light attenuation were much stronger. This negative effect of DOM on phytoplankton biomass was also consistent with an earlier temporal study in the same region (Findlay et al. 2001), and studies reporting the negative effects reported by space-for-time substitutions (Carpenter et al. 1998; Nurnberg and Shaw 1998; Hessen et al. 2017). While we did not assess effects of DOM on benthic algae, space-for-time substitutions using boreal lakes from Sweden (Ask et al. 2009; Karlsson et al. 2009; Seekell et al. 2015) suggest similar or even larger negative effects of DOM on benthic algae and whole-ecosystem productivity. The implications of such changes to benthic algal productivity are likely to be ecologically significant since c. 50% of carbon assimilated by top trophic levels in boreal lakes originate from benthic algal production (Hecky and Hesslein 1995).

While increases in precipitation and lake DOM led to declines in phytoplankton biomass within dimictic lakes over the study period, we found no consistent effect on zooplankton biomass. Two of the dimictic lakes in our dataset (L224, L373) had few records during the 1980s, prior to the rapid increase in precipitation and DOM occurring over subsequent decades. The single lake (L239) with sufficient data throughout the study period showed overall low zooplankton biomass, no significant trends in biomass over time, and there were no significant relationships between DOM and zooplankton biomass within any of the dimictic study lakes. This result is in contrast to an among-lake study in the same region (Tonin et al. 2022), which showed large among-lake declines (c. −70%) in zooplankton biomass as DOM increased from 2.5 to 9.5 mg DOC L^{-1}. The result also contrasts with other space-for-time (i.e., among lake) studies that report similar declines in zooplankton biomass with increasing DOM (Solomon et al. 2015; Hessen et al. 2017; Kelly et al. 2018). However, the result is consistent with studies that have evaluated the response of zooplankton to temporal changes in DOM and found no consistent effect (Williamson et al. 2020; Estlander and Horppila 2023). We speculate that that the low zooplankton biomass in L239 and lack of response to bottom-up pressure associated with reductions in phytoplankton biomass (i.e., their primary food source) occurred because zooplankton biomass in that lake was controlled by top-down pressure (i.e., predation); of the three study lakes L239 was the only lake with a pelagic planktivore (Slongo et al. 2022). A previous among-lake study within the region by Tonin et al. (2022) found that while zooplankton consumed DOM, it was not a subsidy for declines in phytoplankton biomass.

Conclusions

Our results indicated multi-decadal (1980–2019) positive trends in precipitation, DOM and nutrient (TN, TP) loads, and lake DOM concentrations within three dimictic lakes in Canada's boreal forest ecozone (Obj 1.). At an annual scale, precipitation explained most of the variation in DOM and nutrient loads. Temporal increases in lake DOM within the dimictic study lakes were associated with changes to a wide range of physical and chemical variables (K_{d}, I_{mean}, Z_{eu}, V_{eu}, Z_{therm}, TP, TN) and declines in B_{phyto}, but we did not detect long-term declines in B_{zoop} (Obj. 2). Epilimnetic Chl, a commonly used indicator of phytoplankton biomass, was a poor indicator of the response of depth-integrated phytoplankton biomass to DOM and misrepresented the direction and magnitude of effect. However, depth-integrated Chl that was corrected for photoadaptation was strongly correlated with depth-integrated phytoplankton biomass and was a useful indicator of temporal responses to DOM. While improved indicator performance after corrections using Chl:PC ratios were consistent with photoadaptation (i.e., cellular increases in pigment concentration in response to declining water clarity), we cannot rule out community level shifts (i.e., species with different Chl:PC ratios) as the ultimate driver. For zooplankton, the lack of response to DOM suggests either resilience to the smaller changes in DOM within temporal studies compared with space-for-time substitutions, or that zooplankton were under top-down rather than bottom-up controls within these oligotrophic lakes (Obj. 3).

Acknowledgements

We thank the staff of the ELA since 1968 for their dedication, field, and laboratory support. Special thanks to David Schindler, John Shearer, Ken Beaty, Mark Lyng, Mike Stainton, Robert Hecky, Diane Malley, Alex Salki, Steven Page, Ken Sandilands, and Paul Faford for their significant efforts to sustain the long-term monitoring program and early establishment of a LTER database.

Article information

History dates

Received: 14 November 2024
Accepted: 10 June 2025
Accepted manuscript online: 11 July 2025
Version of record online: 2 September 2025

Notes

This paper is part of a Collection entitled Freshwater browning and coastal darkening: effects and processes.

Copyright

Data availability

Data generated or analyzed during this study are available in the Environmental Data Initiative (EDI) repository (https://doi.org/10.6073/pasta/da1b1d8f5e4434125d46762167344675).

Author information

Author ORCIDs

Scott N. Higgins https://orcid.org/0000-0001-9427-7024
Michael J. Paterson https://orcid.org/0000-0002-8526-9126

Author notes

M. Rennie served as Associate Editor at the time of manuscript review and acceptance; peer review and editorial decisions regarding this manuscript were handled by another editorial board member.

Author contributions

Conceptualization: SNH, SMH, MJP, MR
Data curation: SNH, SMH, MJP, PB
Formal analysis: SNH
Investigation: SNH, SMH, MJP
Methodology: SNH, SMH, MJP, PB
Project administration: SNH
Supervision: SNH
Validation: SNH
Visualization: SNH, SMH
Writing – original draft: SNH
Writing – review & editing: SNH, SMH, MJP, MR, PB

Competing interests

The authors declare that they have no competing financial or non-financial interests related to this study.

Funding information

Long-term funding support was provided by operating grants to the ELA from the federal government of Canada and the Province of Ontario.

Supplementary material

Supplementary data are available with the article at https://doi.org/10.1139/cjfas-2024-0341.

References

Ask, J., Karlsson, J., Persson, L., Ask, P., Byström, P., and Jansson, M. 2009. Whole-lake estimates of carbon flux through algae and bacteria in benthic and pelagic habitats of clear-water lakes. Ecology, **90**: 1923–1932. doi:10.1890/07-1855.1. PMID: 19694140.

Hall, B.D., Hesslein, R.H., Emmerton, C.A., Higgins, S.N., Ramlal, P., and Paterson, M.J. 2019. Multidecadal carbon sequestration in a headwater boreal lake. Limnology and Oceanography **64**: S150–S165. doi:10.1002/lno.11060.

Bates, D., Maechler, M., Bolker, B., and Walker, S. 2015. Fitting linear mixed-effects models using lme4. J. Stat. Software, **67**: 1–48. doi:10.18637/jss.v067.i01.

Bayley, S.E., Schindler, D.W., Beaty, K.G., Parker, B.R., and Stainton, M.P. 1992. Effects of multiple fires on nutrient yields from streams draining boreal forest and fen watersheds–nitrogen and phosphorus. Can. J. Fish. Aquat. Sci. **49**: 584–596. doi:10.1139/f92-068.

Carpenter, S.R., Cole, J.J., Kitchell, J.F., and Pace, M.L. 1998. Impact of dissolved organic carbon, phosphorus, and grazing on phytoplankton biomass and production in experimental lakes. Limnol. Oceanogr. **43**: 73–80. doi:10.4319/lo.1998.43.1.0073.

Chang, P.S.S., and Malley, D.F. 1987. Zooplankton in Lake 223, Experimental Lakes Area, Northwestern Ontario 1974-1983. Can. Data Rep. Fish. Aquat. Sci. 665.

Creed, I.F., Bergstrom, A.-K., Trick, C.G., Grimm, N.B., Hessen, D.O., Karlsson, J., et al. 2018. Global change-driven effects on dissolved organic matter composition: implications for food webs of northern lakes. Global Change Biol. **24**: 3692–3714. doi:10.1111/gcb.14129.

de Wit, H.A., Stoddard, J.L., Monteith, D.T., Sample, J.E., Austnes, K., Couture, S., et al. 2021. Cleaner air reveals growing influence of climate on dissolved organic carbon trends in northern headwaters. Environ. Res. Lett. 16. doi:10.1088/1748-9326/ac2526.

Diodato, N., Higgins, S., Bellocchi, G., Fiorillo, F., Romano, N., and Guadagno, F.M. 2016. Hydro-climatic forcing of dissolved organic carbon in two boreal lakes of Canada. Sci. Total Environ. **571**: 50–58. doi:10.1016/j.scitotenv.2016.07.112. PMID: 27459253.

Downing, J., Prairie, Y., Cole, J., Duarte, C., Tranvik, L., Striegl, R., et al. 2006. The global abundance and size distribution of lakes, ponds, and impoundments. Limnol. Oceanogr. **51**: 2388–2397. doi:10.4319/lo.2006.51.5.2388.

Emmerton, C.A., Beaty, K.G., Casson, N.J., Graydon, J.A., Hesslein, R.H., Higgins, S.N., et al. 2019. Long-term responses of nutrient budgets to concurrent climate-related stressors in a boreal watershed. Ecosystems, **22**: 363–378. doi:10.1007/s10021-018-0276-7.

Erlandsson, M., Buffam, I., Fölster, J., Laudon, H., Temnerud, J., Weyhenmeyer, G.A., and Bishop, K. 2008. Thirty-five years of synchrony in the organic matter concentrations of Swedish rivers explained by variation in flow and sulphate. Global Change Biol. **14**: 1191–1198. doi:10.1111/j.1365-2486.2008.01551.x.

Estlander, S., and Horppila, J. 2023. Effects of dissolved organic carbon gradient on epilimnetic zooplankton communities in lakes. Hydrobiologia, **850**: 4015–4027. doi:10.1007/s10750-023-05284-6.

Fee, E.J., Hecky, R.E., Kasian, S.E.M., and Cruikshank, D.R. 1996. Effects of lake size, water clarity, and climatic variability on mixing depths in

Canadian Shield lakes. Limnol. Oceanogr. **41**: 912–920. doi:10.4319/lo.1996.41.5.0912.

Findlay, D.L., Kasian, S.E.M., Stainton, M.P., Beaty, K., and Lyng, M. 2001. Climatic influences on algal populations of boreal forest lakes in the Experimental Lakes Area. Limnol. Oceanogr. **46**: 1784–1793. doi:10.4319/lo.2001.46.7.1784.

Francko, D.A. 1986. Epilimnetic phosphorus cycling–influence of humic materials and iron on coexisting major mechanisms. Can. J. Fish. Aquat. Sci. **43**: 302–310. doi:10.1139/f86-039.

Guzzo, M.M., and Blanchfield, P.J. 2017. Climate change alters the quantity and phenology of habitat for lake trout (Salvelinus namaycush) in small Boreal Shield lakes. Can. J. Fish. Aquat. Sci. **74**: 871–884. doi:10.1139/cjfas-2016-0190.

Havens, S.M., Cooney, B.T., and Stainton, M.P. 2024. The chemical analysis of freshwater. 3rd ed. International Institute for Sustainable Development, Winnipeg, Canada. doi:10.13140/RG.2.2.32178.82889.

Heathcote, A.J., Anderson, N.J., Prairie, Y.T., Engstrom, D.R., and Del Giorgio, P.A. 2015. Large increases in carbon burial in northern lakes during the Anthropocene. Nat. Commun. **6**. doi:10.1038/ncomms10016. PMID: 26607672.

Hecky, R.E., and Hesslein, R.H. 1995. Contributions of benthic algae to lake food webs as revealed by stable isotope analysis. J. North Am. Benthological Soc. **14**: 631–653. doi:10.2307/1467546.

Hessen, D.O., Hall, J.P., Thrane, J.-E., and Andersen, T. 2017. Coupling dissolved organic carbon, CO2 and productivity in boreal lakes. Freshwater Biol. **62**: 945–953. doi:10.1111/fwb.12914.

Higgins, S.N., Desjardins, C.M., Drouin, H., Hrenchuk, L.E., and van der Sanden, J.J. 2021. The role of climate and lake size in regulating the ice phenology of boreal lakes. J. Geophys. Res. Biogeosci. 126. doi:10.1029/2020jg005898.

Hothorn, T., Bretz, F., and Westfall, P. 2008. Simultaneous inference in general population models. Biom. J. **50**: 346–363. doi:10.1002/bimj.200810425. PMID: 18481363.

Imtiazy, M.N., Paterson, A.M., Higgins, S.N., Yao, H., Houle, D., and Hudson, J.J. 2025. Has brownification ceased? Stabilization, rebrowning, and other factors associated with dissolved organic matter trends in eastern Canadian lakes. Water Res. **269**: 122814. doi:10.1016/j.watres.2024.122814. PMID: 39581116.

IPCC. 2023. Climate change 2023: synthesis report. *In* Contribution of working groups I, II and III to the sixth assessment report of the Intergovernmental Panel on Climate Change. *Edited by* Core writing team, H. Lee and J. Romero. doi:10.59327/IPCC/AR6-9789291691647.

Isles, P.D.F., Creed, I.F., Jonsson, A., and Bergstrom, A.-K. 2021. Trade-offs between light and nutrient availability across gradients of dissolved organic carbon lead to spatially and temporally variable responses of Lake phytoplankton biomass to browning. Ecosystems, **24**: 1837–1852. doi:10.1007/s10021-021-00619-7.

Jackson, T.A., and Hecky, R.E. 1980. Depression of primary productivity by humic matter in lake and reservoir waters of the boreal forest zone. Can. J. Fish. Aquat. Sci. **37**: 2300–2317. doi:10.1139/f80-277.

Johannsson, O.E., Shaw, M., Yan, N.D., Filion, J.M., and Malley, D.F. 1992. A comparison of freshwater zooplankton sampling gear: nets, traps, and submersible pump. Can. Tech. Rep. Fish. Aquat. Sci. 1894.

Jones, R.I. 1992. The influence of humic substances on lacustrine planktonic food-chains. Hydrobiologia, **229**: 73–91. doi:10.1007/bf00006992.

Karlsson, J., Bystrom, P., Ask, J., Ask, P., Persson, L., and Jansson, M. 2009. Light limitation of nutrient-poor lake ecosystems. Nature, **460**: 506–U80. doi:10.1038/nature08179. PMID: 19626113.

Kelly, P.T., Solomon, C.T., Zwart, J.A., and Jones, S.E. 2018. A framework for understanding variation in pelagic gross primary production of lake ecosystems. Ecosystems, **21**: 1364–1376. doi:10.1007/s10021-018-0226-4.

Kruskopf, M., and Flynn, K.J. 2006. Chlorophyll content and fluorescence responses cannot be used to gauge reliably phytoplankton biomass, nutrient status or growth rate. New Phytol. **169**: 525–536. doi:10.1111/j.1469-8137.2005.01601.x. PMID: 16411955.

Lenth, R. 2024. Estimated marginal means, aka least-squares means. R package version 1.10.4. Available from https://CRAN.R-project.org/package=emmeans.

Malley, D.F., Lawrence, S.G., Maciver, M.A., and Findlay, W.J. 1989. Range of variation in estimates of dry weight for planktonic crustacea and rotifera from temperate North America lakes. Can. Tech. Rep. Fish. Aquat. Sci. 1666.

Maranger, R., and Pullin, M. 2003. Elemental complexation by dissolved organic matter in lakes: implications for Fe speciation and the speciation and the bioavailability of Fe and P. *In* Aquatic ecosystems: interactivity of dissolved organic matter. *Edited by* S. Findlay and R. Sinsabaugh. Academic Press, New York. doi:10.1016/B978-012256371-3/50009-3.

Mcleod, A. 2022. Kendall: Kendal rank correlation and Mann-Kendall trend test. R package version 2.2.1. Available from https://CRAN.R-project.org/package=Kendall [accessed July 2023].

Meyer-Jacob, C., Michelutti, N., Paterson, A.M., Cumming, B.F., Keller, W., and Smol, J.P. 2019. The browning and re-browning of lakes: divergent lake-water organic carbon trends linked to acid deposition and climate change. Sci. Rep. **9**. doi:10.1038/s41598-019-52912-0.

Molot, L.A., Higgins, S.N., Schiff, S.L., Venkiteswaran, J.J., Paterson, M.J., and Baulch, H.M. 2021. Phosphorus-only fertilization rapidly initiates large nitrogen-fixing cyanobacteria blooms in two oligotrophic lakes. Environ. Res. Lett. **16**. doi:10.1088/1748-9326/ac0564.

Monteith, D.T., Henrys, P.A., Hruska, J., de Wit, H.A., Krám, P., Moldan, F., et al. 2023. Long-term rise in riverine dissolved organic carbon concentration is predicted by electrolyte solubility theory. Sci. Adv. 9. doi:10.1126/sciadv.ade3491.

Monteith, D.T., Stoddard, J.L., Evans, C.D., de Wit, H.A., Forsius, M., Hogasen, T., et al. 2007. Dissolved organic carbon trends resulting from changes in atmospheric deposition chemistry. Nature, **450**: 537–540. doi:10.1038/nature06316. PMID: 18033294.

Nauwerk, A. 1963. Beziechungen Zwischen Zooplankton und Phytotoplankton in see Erken. Symb. Bot. **17**: 1–163.

Nurnberg, G.K., and Shaw, M. 1998. Productivity of clear and humic lakes: nutrients, phytoplankton, bacteria. Hydrobiologia, **382**: 97–112. doi:10.1023/a:1003445406964.

Parker, B.R., Schindler, D.W., Beaty, K.G., Stainton, M.P., and Kasian, S.E.M. 2009. Long-term changes in climate, streamflow, and nutrient budgets for first-order catchments at the Experimental Lakes Area (Ontario, Canada). Can. J. Fish. Aquat. Sci. **66**: 1848–1863. doi:10.1139/f09-149.

Paterson, M.J., Schindler, D.W., Hecky, R.E., Findlay, D.L., and Rondeau, K.J. 2011. Comment: Lake 227 shows clearly that controlling inputs of nitrogen will not reduce or prevent eutrophication of lakes. Limnol. Oceanogr. **56**: 1545–1547. doi:10.4319/lo.2011.56.4.1545.

Pohlert, T. 2023. Trend: non-parametric trend tests and change-point detection. R package version 1.1.6. Available from https://CRAN.R-project.org/package=trend [accessed July 2023].

Salki, A. 1993. Lake variation and climate change study: VII. Crustacean plankton of a lake flushing rate series in the Experimental Lakes Area, Northwestern Ontario, 1987-1990. Can. Data Rep. Fish. Aquat. Sci. 880.

Schindler, D., and Fee, E. 1974. Experimental Lakes Area: whole-lake experiments in eutrophication. J. Fish. Res. Board Can. **31**: 937–953. doi:10.1139/f74-110.

Schindler, D.W., Bayley, S.E., Parker, B.R., Beaty, K.G., Cruikshank, D.R., Fee, E.J., et al. 1996. The effects of climatic warming on the properties of boreal lakes and streams at the Experimental Lakes Area, Northwestern Ontario. Limnol. Oceanogr. **41**: 1004–1017. doi:10.4319/lo.1996.41.5.1004.

Seekell, D.A., Lapierre, J.-F., Ask, J., Bergstroem, A.-K., Deininger, A., Rodriguez, P., and Karlsson, J. 2015. The influence of dissolved organic carbon on primary production in northern lakes. Limnol. Oceanogr. **60**: 1276–1285. doi:10.1002/lno.10096.

Senar, O.E., Creed, I.F., and Trick, C.G. 2021. Lake browning may fuel phytoplankton biomass and trigger shifts in phytoplankton communities in temperate lakes. Aquat. Sci. 83. doi:10.1007/s00027-021-00780-0.

Shearer, J.A. 1978. Devices for obtaining water samples integrated over depth. Can. Fish. Mar. Serv. Tech. Rep. 1–9.

Sherbo, B.A.H., Tonin, J., Paterson, M.J., Hann, B.J., Kozak, J., and Higgins, S.N. 2023. The effects of terrestrial dissolved organic matter on phytoplankton biomass and productivity in boreal lakes. Freshwater Biol. **68**: 2109–2119. doi:10.1111/fwb.14178.

Slongo, B.D., Hayhurst, L.D., Drombolis, P.C.T., Metcalfe, C.D., and Rennie, M.D. 2022. Whole-lake nanosilver additions reduce northern pike (*Esox lucius*) growth. Sci. Total Environ. 838. doi:10.1016/j.scitotenv.2022.156219.

Solomon, C.T., Jones, S.E., Weidel, B.C., Buffam, I., Fork, M.L., Karlsson, J., et al. 2015. Ecosystem consequences of changing inputs of terrestrial dissolved organic matter to lakes: current knowledge and future challenges. Ecosystems, **18**: 376–389. doi:10.1007/s10021-015-9848-y.

Stetler, J.T., Knoll, L.B., Driscoll, C.T., and Rose, K.C. 2021. Lake browning generates a spatiotemporal mismatch between dissolved organic carbon and limiting nutrients. Limnol. Oceanogr. Lett. **6**: 182–191. doi:10.1002/lol2.10194.

Tonin, J.A., Rennie, M.D., Higgins, S.N., and Paterson, M.J. 2025. Dissolved organic carbon suppresses benthivorous fish biomass by mediating benthic invertebrate resources. Can. J. Fish. Aquat. Sci. **82**: 1–11. doi:10.1139/cjfas-2024-0338.

Tonin, J.A., Sherbo, B., Higgins, S.N., Schiff, S.L., and Paterson, M.J. 2022. Dissolved organic carbon affects the occurrence of deep chlorophyll peaks and zooplankton resource use and biomass. Freshwater Biol. **67**: 1357–1369. doi:10.1111/fwb.13922.

Verpoorter, C., Kutser, T., Seekell, D.A., and Tranvik, L.J. 2014. A global inventory of lakes based on high-resolution satellite imagery. Geophys. Res. Lett. **41**: 6396–6402. doi:10.1002/2014GL060641.

Vollenweider, R.A. 1968. Scientific fundamentals of the eutrophication of lakes and flowing waters, with particular reference to nitrogen and phosphorus as factors in eutrophication. Tech. Rep. O.E.C.D. Paris Das/CS1/68.27.

Webster, K.E., Soranno, P.A., Cheruvelil, K.S., Bremigan, M.T., Downing, J.A., Vaux, P.D., et al. 2008. An empirical evaluation of the nutrient-color paradigm for lakes. Limnol. Oceanogr. **53**: 1137–1148. doi:10.4319/lo.2008.53.3.1137.

Weyhenmeyer, G.A., Müller, R.A., Norman, M., and Tranvik, L.J. 2016. Sensitivity of freshwaters to browning in response to future climate change. Clim. Change, **134**: 225–239. doi:10.1007/s10584-015-1514-z.

Williamson, C.E., Morris, D.P., Pace, M.L., and Olson, A.G. 1999. Dissolved organic carbon and nutrients as regulators of lake ecosystems: resurrection of a more integrated paradigm. Limnol. Oceanogr. **44**: 795–803. doi:10.4319/lo.1999.44.3_part_2.0795.

Williamson, C.E., Overholt, E.P., Pilla, R.M., and Wilkins, K.W. 2020. Habitat-mediated responses of zooplankton to decreasing light in two temperate lakes undergoing long-term browning. Front. Environ. Sci. **8**. doi:10.3389/fenvs.2020.00073.

Zeileis, A., Keliber, C., Kramer, W., and Hornik, K. 2003. Struccchange: an R package for testing for structural changes in linear regression models. J. Stat. Software, **7**: 1–38. doi:10.18637/jss.v007.i02.